Asian Journal of Chemistry; Vol. 38, No. 3 (2026), 619-628
ASIAN JOURNAL OF CHEMISTRY
https://doi.org/10.14233/ajchem.2026.35190

Isolation and Structural Characterization of (-)-Epicatechin from *Cassia fistula* L. Seeds: *In Silico* Docking and ADMET Profiling for the Evaluation of Antiepileptic Potential Targeting $GABA_A$ Receptor

VIJAYAVILAS SATHYAN SANGEETHA[1,*], P. CHRISTINA RUBY STELLA[2,*], V. PRIYA[3] and NIVETHA ARUNPRAKASH[3]

[1]Department of Chemistry, Dhanalakshmi Srinivasan College of Arts and Science for Women (Autonomous) (Affiliated to Bharathidasan University, Tiruchirapalli), Perambular-621212, India
[2]Department of Science and Humanities, Sri Vignesh College of Engineering and Technology, Tiruchirapalli-621216, India
[3]Department of Chemistry, Holy Cross College (Affiliated to Bharathidasan University, Tiruchirapalli), Tiruchirapalli-620002, India

*Corresponding author: E-mail: sangeethavasanth23@gmail.com

Received: 4 November 2025 *Accepted*: 23 December 2025 *Published online*: 6 March 2026 AJC-22280

The current experimental study is concerned with the isolation of epicatechin, a naturally occurring flavonoid, from the seed of *Cassia fistula* L and to investigate the biological potential by executing molecular docking studies against the $GABA_A$ receptor, a crucial target in neuropharmacology that moderates the signaling in the central nervous system (CNS). The physico-chemical, pharmacokinetic and pharmacodynamic properties of epicatechin were evaluated; validate its drug-like characteristics and support its potential as therapeutic agent against CNS related disorders. Molecular docking analysis revealed a favourable interaction between epicatechin and the $GABA_A$ receptor, suggesting its potential as a selective therapeutic candidate. The calculated binding affinity of epicatechin (-5.204 kcal/mol) was stronger than that of the reference ligand diazepam (-4.216 kcal/mol), indicating a comparatively more stable ligand–receptor complex. These findings imply that epicatechin may effectively modulate the GABAergic pathway through energetically favourable binding interactions within the receptor's active site and exhibit significant antiepileptic efficacy. This experimental approach incorporates traditional isolation and purification methods with computational drug target techniques, which come up with new insights into the pharmaceutical potential of *Cassia fistula* L.

Keywords: Epicatechin, γ-Aminobutyric acid, Central neural system, Chromatography, Isolation, Molecular docking.

INTRODUCTION

Medicinal plants have long served as a vital reservoir for pharmaceutical compounds and therapeutic agents, dating back to ancient civilisations. These natural resources offer a wide spectrum of treatments for various ailments and their significance in traditional and modern medicine continues to be reaffirmed through ongoing scientific investigations [1-5]. Contemporary research frequently validates the traditional use of plant-based remedies, providing a scientific foundation for their efficacy in managing human diseases [6,7]. A considerable number of pharmacologically active compounds used today are derived from secondary metabolites produced by medicinal plants [8]. The therapeutic potent constituents isolated from medicinal plants usually possess compounded chemical structures and reveal significant biological activities, making them strong candidates for drug invention aimed at inhibit severe and chronic conditions [9-11]. Many of these natural occurring secondary metabolites have shown potential in managing neurological and neuromuscular disorders. Moreover, various phytochemicals have revealed immunomodulatory activities, playing a key role in regulating and elevating immune system functions [12,13].

Extensive efforts in natural product research led to the isolation and identification of multitude of drug-like molecule over the past few decades, leading to new structural classes and also unveiled mechanism of action, enriching the drug discovery pipeline [14]. In the group of various medicinal plants studied, *Cassia fistula* L., often known as the golden shower tree, has secured attention for its numerous pharmacological potential [15,16]. This plant is employed as Ayurvedic medicine and utilised in several traditional healing systems.

This plant extract has been utilised to treat various health issues such as, diabetes, hematemesis, leukoderma (vitiligo), pruritus (itchiness), erysipelas (a class of skin infection) and dermatological disorders [17]. The extracts of *C. fistula* L. have been traditionally employed in the therapy of bone fractures [18]. Empirical studies have also highlighted its antioxidant properties, signifying its role in preventing oxidative stress and hence reducing cellular damage [19]. Collectively, these findings underscore the importance of plant-derived natural products as valuable sources for developing safe and innovative therapeutics. Exploration of their bioactive compounds holds strong potential for managing both existing and emerging health challenges. The plant has been reported to improve liver function [20], exhibit cytotoxic properties, regulate cholesterol levels [21], and reduce insulin resistance [22].

Among the bioactive phytochemicals, flavonoids, in particular, are acknowledged as best contributors to the pharmacological activities of several medicinal plants. They possess a key role in mediating numerous biochemical pathways and have been extensively investigated for their versatile pharmacological properties as well as therapeutic properties [23-25]. Furthermore, flavonoids are well known for their potent antioxidant capacity. By scavenging free radicals and limiting oxidative stress, they help safeguard essential biomolecules such as DNA, proteins and lipids from damage [26-28]. This protective mechanism plays a significant role in delaying or preventing the progression of degenerative diseases, including cardiovascular and neurodegenerative disorders, as well as certain cancers [29].

The search for novel neuroleptic GABAergic agents derived from plant secondary metabolites aims to produce safe and effective therapeutics for the management of central nervous system (CNS)-related disorders. The finding of this investigation highlights efficacy of epicatechin, the plant-derived flavonoid form *C. fistula* L., as a potential GABAergic signaling modulator with a high affinity and docking score and notable pharmacological properties for managing epilepsy.

EXPERIMENTAL

All solvents, reagents and analytical grade chemicals used in this study were procured from reputable chemical suppliers. *Cassia fistula* L. seeds were carefully collected, when the cylindrical, long seed pods turned dark brown (dry pods) and produce rattling sound when shaken, from the selected areas of Perambalur district, India. The cleaned plant seeds were subjected to a shade-drying process to preserve heat sensitive phytochemicals. Once after fully dried, the seeds were ground into a fine powder using a mechanical blender and processed for experimental use.

Characterization: The isolated compound was characterized using several spectroscopic techniques, namely UV-Vis, FT-IR and $^{1}H/^{13}C$ NMR spectroscopy. The UV-Vis analysis was performed on a Shimadzu 160A spectrophotometer. FT-IR spectra were recorded using the KBr pellet method over the range of 4000-400 cm^{-1} with a resolution of 4 cm^{-1}. The ^{1}H and ^{13}C NMR spectra were obtained on Bruker WP 200SY and AM 200SY instruments, employing $CDCl_3$ as the solvent and tetramethylsilane (TMS) as the internal reference.

Isolation by column chromatography over preparative TLC: The isolation process was performed on a concentrated ethanol extract (50 g) of *C. fistula* L., using column chromatography over silica gel with a gradient of solvents in order of increasing polarity. Elution initiated with solvent *n*-hexane, then by mixtures of ethyl acetate and *n*-hexane and eventually with methanol, resulting in the collection of multiple fractions. To ensure thorough extraction, the procedure was repeated. Epicatechin was successfully isolated from fraction 23 using a solvent system composed of ethyl acetate and methanol in a 70:30 ratio. The isolated compounds were detected on preparative thin-layer chromatography (TLC) plates using Liebermann-Burchard reagent and at a subsequent time heated at 100 ºC to facilitate detection.

Optimisation of HPTLC chromatographic conditions: HPTLC fingerprint patterns have been analysed for the sample to evaluate the phytochemical profile. The study was performed on HPTLC pre-coated silica gel 60 F_{254} plates (E. Merck) plate with a flat thickness of 0.2 mm. A solvent system of toluene:ethyl acetate:methanol:acetic acid (2.7:6:1:0.3) was employed as the mobile phase to determine the R_f value and retention time of the isolated compound, followed by comparison with standard epicatechin. Aliquots of 5 µL of standard solution (S1) and 5 µL and 10 µL of test solutions (T1 and T2) were spotted onto the HPTLC plate using a CAMAG Linomat 5 sample applicator. The plate was then developed in the selected prepared solvent system. After development, the chromatogram was scanned densitometrically at 254 nm using a CAMAG TLC Scanner 3. Observation of the formed spots was performed using ultraviolet light at 254 nm and 366 nm wavelength using a CAMAG Reprostar 3 documentation system.

Molecular docking: In this study the receptor grid was prepared utilizing standard settings in glide with employing the co-crystallised binder molecule to specify the core of the grid box. Molecular docking was executed to assess the binding interaction procedure, linking the target protein and the selected drug molecule, also to investigate their interaction modes. Ligand-protein docking was executed by utilizing the extra precision (XP) mode to assure validity and constancy of the anticipated binding interactions. Standard docking parameters were employed and the linking analogy of the resulting receptor-drug was analysed using glide's scoring functions. The scores hence analysed contribute insights into the intensity and nature of the binding interactions; promote the recognition of the most able drug candidates for further research.

Data acquisition: The three-dimensional structure of the target GABA (γ-amino butyric acid) receptor was retrieved from the Protein Data Bank (PDB ID: 8BHK), with a reported crystallographic resolution of 3.30 Å. The molecular structures of diazepam and epicatechin were obtained from publicly available chemical databases, namely PubChem and ZINC (https://zinc.docking.org/), and subsequently prepared for the computational analysis.

Ligand preparation: The selected ligands were prepared using the LigPrep unit of the Schrödinger suite. This tool converts 2-dimentional (2D) chemical structures or conformers of ligands into optimised 3-dimentional (3D) conformers and also produce proper tautomeric and ionisation states. Each ligand candidate structure was conformer-enhanced empl-

oying the OPLS3e force field; confirm precise bond lengths, angles and conformational flexibility in advance to docking.

Protein preparation: Protein preparation was carried out using the Protein Preparation Wizard implemented in the Schrödinger suite. The three-dimensional crwystal structure of the receptor was imported into the Maestro workspace and subjected to standard preprocessing. Missing residues and side chains were modeled using the Prime module. Hydrogen bond optimization was performed with the H-bond assignment tool and water molecules located beyond 3.0 Å from the active site were removed to avoid interference during docking. Prior to docking, the receptor structure underwent energy minimization using the OPLS3 force field to relieve steric strain and stabilize the geometry. This procedure ensured a properly optimized and energetically favourable protein conformation suitable for accurate molecular docking analysis.

ADMET property prediction: The ADMET properties of diazepam and epicatechin were analysed with the help of the QikProp module in Schrödinger software. These property predictions were carried out based on the available information about structural and physico-chemical properties of each ligand species. The physico-chemical parameters of the drug candidates including molecular weight (MW), partition coefficient ($QlogP_o/w$) and solvent-accessible surface area (SASA), were accessed. In addition, pharmacokinetic properties were analysed, like serum protein binding capability (QlogKhsa), blood-brain barrier permeability (QlogBB) and intestinal absorption utilizing MDCK cell line permeability (QPP MDCK). These assessments were required in discover the drug-likeness and pharmaceutical viability of the drug candidates.

RESULTS AND DISCUSSION

Collection of plant materials: *Cassia fistula* L. seeds were carefully collected, when the cylindrical, long seed pods turned dark brown (dry pods) and produce rattling sound when shaken, from the selected areas of Perambalur district, India. The cleaned plant seeds were subjected to a shade-drying process to preserve heat sensitive phytochemicals. Once after fully dried, the plant seeds were ground into a fine powder using a mechanical blender and processed for experimental use.

Quantitative analysis: A quantitative evaluation of the ethanolic seed extract of *C. fistula* L. was conducted to determine the levels of major bioactive constituents, including flavonoids, phenols, tannins, alkaloids, terpenoids and saponins. Quantification was performed using standardized spectrophotometric and gravimetric methods, and the results were expressed as mg/g of dried extract. The estimated concentrations were to be as flavonoids (0.008 mg/g), phenols (0.007 mg/g), tannins (0.006 mg/g), alkaloids (0.005 mg/g), terpenoids (0.004 mg/g) and saponins (0.003 mg/g). Based on these results, flavonoids are present in the highest amount among the analyzed constituents, indicating a predominance of antioxidant-associated compounds in the extract. The presence of other phytochemical classes, though comparatively lower, also supports the broad therapeutic potential of the seed extract [30-32].

Isolation by column chromatography: The crude ethanolic extract of *C. fistula* L. seeds (50 g) was subjected to silica gel column chromatography to isolate the target phytoconstituent. Elution was carried out using a stepwise polarity gradient, beginning with *n*-hexane, followed by increasing proportions of ethyl acetate in *n*-hexane and finally methanol. Fractions were collected sequentially during the separation process. The 23rd fraction contained a prominent compound, which was further purified using a binary solvent system of ethyl acetate and methanol (70:30). Purity assessment was performed by preparative thin-layer chromatography (TLC). The isolated compound showed a distinct spot with a R_f value of 0.63 and a peak area of 0.81%, consistent with the standard epicatechin reference [33].

Identification and quantification of epicatechin using TLC and HPTLC: The isolated compound exhibited an R_f value of 0.58, when measured using HPTLC, consistent with that of the reference epicatechin standard. The retention time was recorded at approximately 3.865 min, confirming successful isolation from the *C. fistula* L. seed extract. The close agreement in chromatographic parameters between the test sample and the standard supports both the identity and purity of the isolated compound. Fig. 1 presents the developed chromatograms of the standard and isolated epicatechin, demonstrating clear peak alignment and effective separation.

Characterisation of isolated epicatechin: The compound isolated from the ethanolic seed extract of *C. fistula* L. was characterized through physico-chemical and spectroscopic evaluation to establish its identity as epicatechin, a recognized flavonoid. It appeared as a light brown crystalline solid with a melting point of 238-239 ºC, closely matching reported values and indicating high purity. The molecular weight was determined to be 290.08 g/mol, corresponding to the molecular formula $C_{15}H_{15}O_6$ and confirming the expected composition. The HPLC chromatogram of the purified compound (Fig. 2) shows a single sharp peak, further supporting its purity and successful isolation.

The UV-absorption spectrum of the isolated epicatechin was recorded in methanol, revealed two absorption maxima (λ_{max}) at 226.8 nm and 279.9 nm as shown in Fig. 3. These bands are characteristic of conjugated π–electrons systems and suggest the existence of aromatic rings and phenolic chromophores. The ~279.9 nm peak is typically associated with the flavonoid B-ring, whereas the 226.8 nm absorption band corresponding to benzoyl system (A-ring), collectively confirming the expected UV pattern of flavonoid-type structures such as epicatechin.

The FT-IR spectroscopy was performed to identify the functional groups present in the isolated compound. The obtained spectrum exhibited characteristic absorption bands typical of a flavonoid framework, confirming the presence of functional groups consistent with the molecular structure of epicatechin. A broad intense peak at 3421 cm^{-1} corresponds to O–H stretching vibrations, suggesting the presence of multiple hydroxyl groups that are typical of flavonoid compounds [34]. The absorption band at 2930 cm^{-1} is assign to C–H stretching vibrations, stand for both aliphatic and aromatic hydrogen atoms. A moderate intense band at 1388 cm^{-1} is attributed to the aromatic ring deformations or phenolic O–H bending (Fig. 4), while the peak present in 1259 cm^{-1} region corresponds to C–O stretching, also supporting the existence of phenolic and ether functionalities. Collectively, these spectral features align with known chemical features of epicatechin.

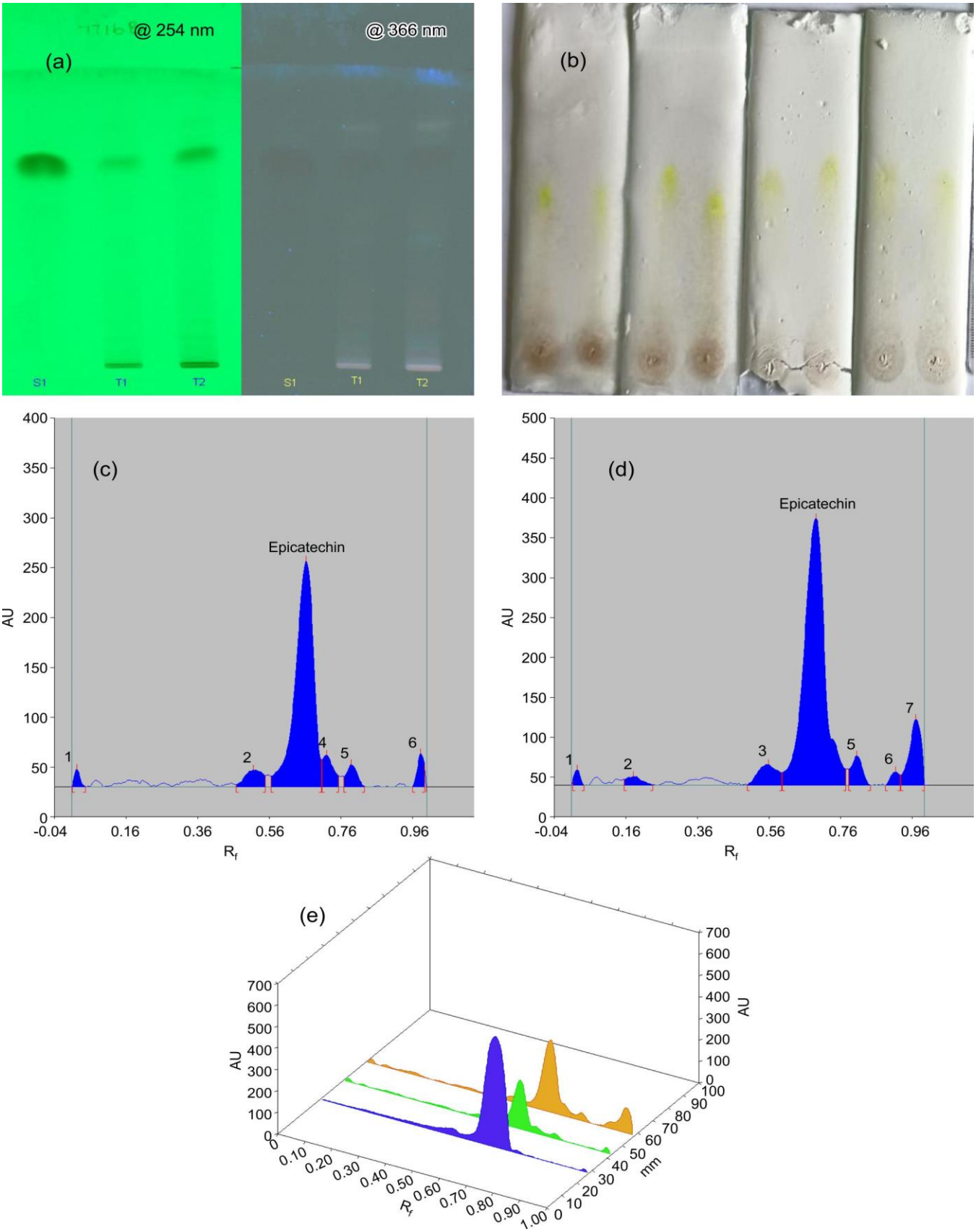

Fig. 1. (a) HPTLC of standard and isolated epicatechin @ 254 nm and @ 366 nm, (S1- standard Epicatechin solution; T1-test solution (5 µL) of Cassia fistula and T2- test solution (10 µL) of Cassia fistula, (b) TLC for isolated compounds, (c) peak display (5 µL of test solution T1), (d) peak display (10 µL of test solution T2) and (e) 3D display @ 254 nm

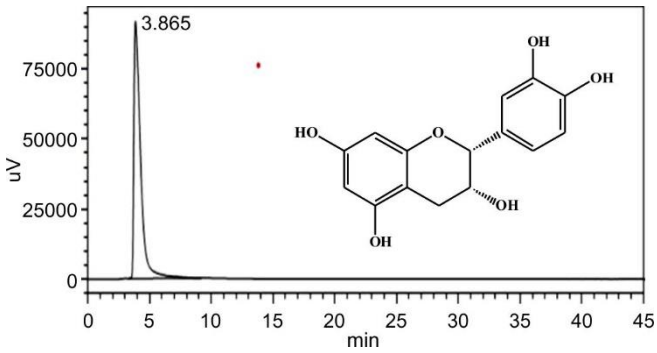

Fig. 2. HPLC chromatogram of epicatechin

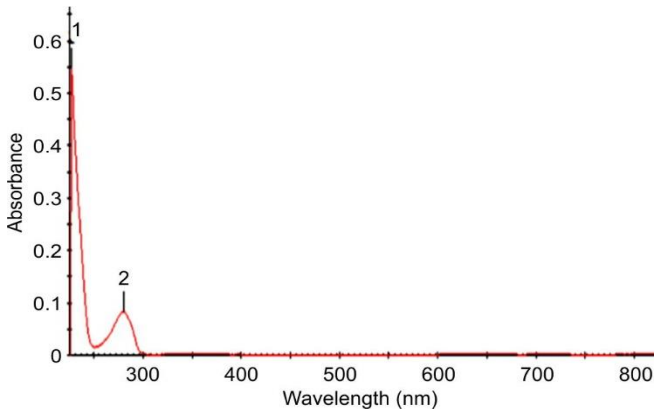

Fig. 3. UV-Vis spectrum of isolated epicatechin

The ^{1}H NMR spectrum of the isolated epicatechin in CD_3OD is shown in Fig. 5a. The characteristic resonance signals consistent with structure of epicatechin, a flavan-3-ol. The A-ring aromatic protons seem as two *meta*-coupled doublets at δ 5.888 (1H, d, *J* = 2.2 Hz, H-8), δ 5.862 (1H, d, *J* = 2.2 Hz. H-6), confirming a 5,7-dihydroxy substitution pattern. The B-

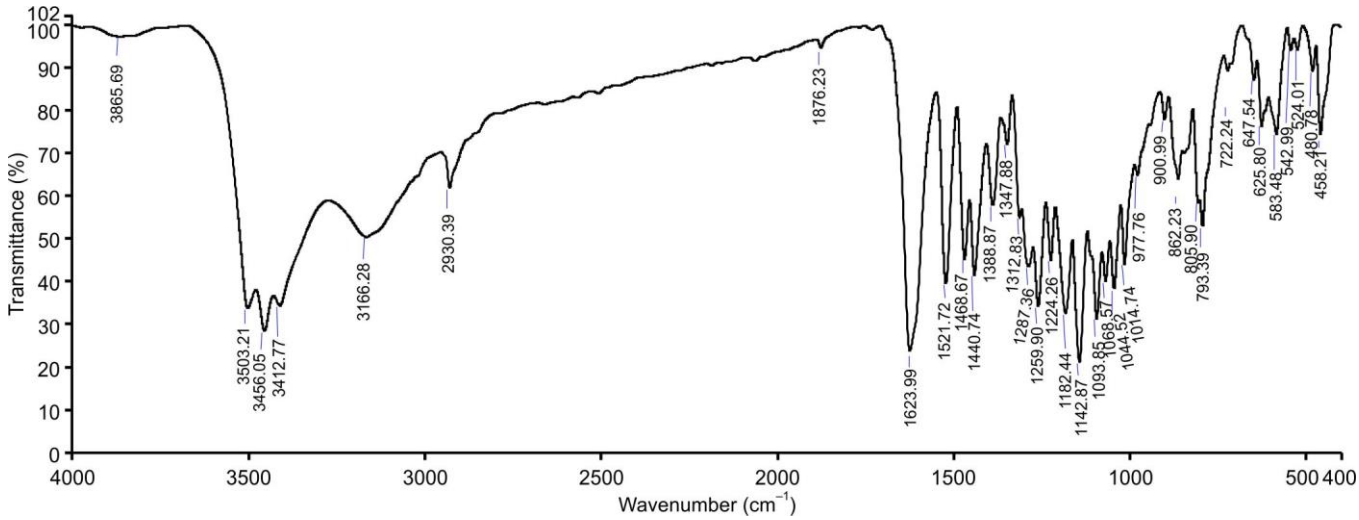

Fig. 4. FT-IR spectrum of isolated epicatechin

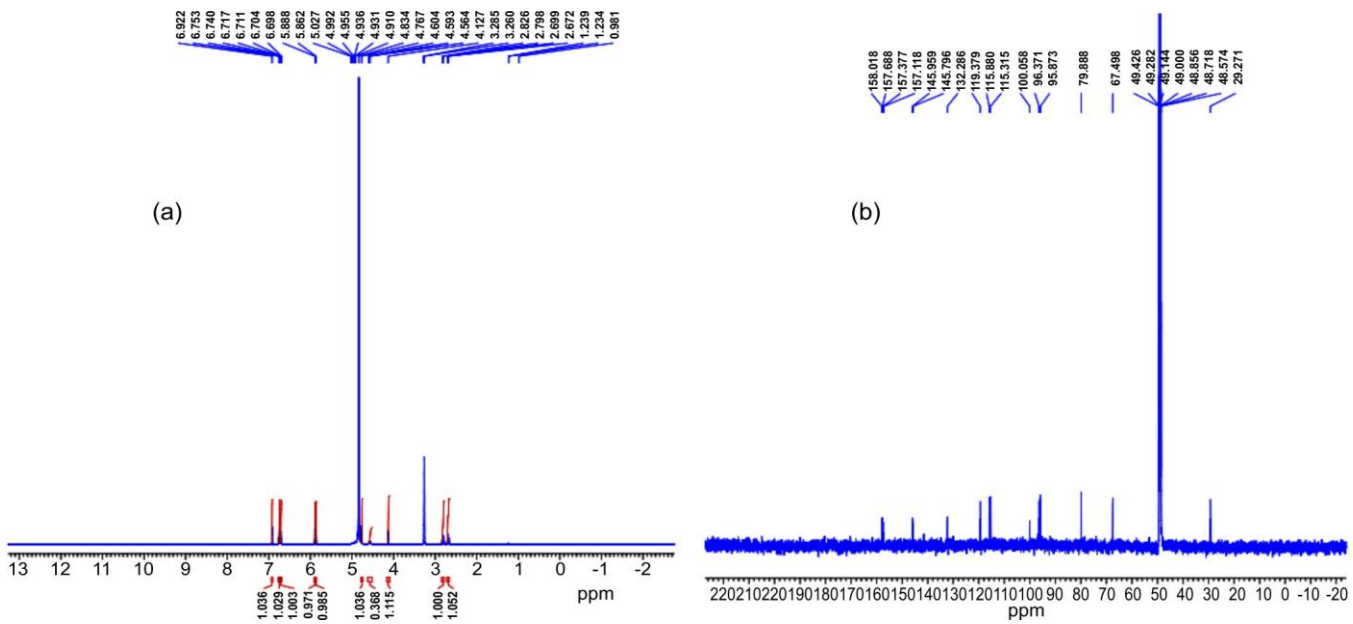

Fig. 5. (a) ^{1}H NMR (in CD_3OD) and (b) ^{13}C NMR spectrum of isolated epicatechin

ring protons from an ABX pattern system observe at δ 6.922 (1H, d, *J* = 1.7 Hz, H-2′), δ 6.753 (1H, dd, *J* = 1.8, 8.5 Hz, H-6′) and δ 6.740 (1H, d, 8.5 Hz, H-5′), consistent with a 3′,4′-dihydroxy arrangement. The aliphatic region possesses significant signals of the heterocyclic C-ring. A broad singlet at δ 4.834 (1H, brs) corresponds to H-2,a multiplet at δ 4.127 (1H, m) represent H-3 and a couple of double doublet at δ 2.798 (1H, dd, *J* = 3.3, 16.7 Hz) and δ 2.826 (IH, dd, *J* = 4.6, 16.7 Hz) attributed to the diastereotopic proton H-4a and H-4b. Together confirm the flavan-3-ol skeleton of epicatechin.

The ^{13}C NMR (600 MHz, CD_3OD) spectrum of isolated compound is illustrated in Fig. 5b, displaying signals for all 15 carbons, further confirms the structure of epicatechin. Significantly, the oxygenated aromatic carbons resonate at δ 157.118 (C-5), δ 157.377 (C-7) and δ 157.688 (C-9). Whereas the C-ring aliphatic carbons appear at δ 79.888 (C-2), 67.498 (C-3), 29.271 (C-4). The B-ring aromatic carbons such as oxygenated C-3′ and C-4′ atoms appear at δ 145.796 and δ 145.959, respectively. Other carbons are resonated at δ 96.371 (C-10), δ 96.371 (C-6), δ 95.873 (C-8), δ 132.286 (C-1′), δ 115.880 (C-2′), δ 119.379 (C-6′) and δ 115.315 (C-5′), respectively. Thus, these data support the identity of the isolated compound as epicatechin align with reported spectral values [35].

ADMET properties: A comprehensive assessment of the Pharmacokinetic and physico-chemical properties of diazepam and epicatechin was prepared to assess their potential as CNS active drug candidate and the result are presented as in Table-1. An initial set of 45 ADMET related properties was initially analysed using QikProp, a widely used predictive tool. From these parameters, specified nine key parameters were selected for detailed discussion on the drug-likeness of molecules based on their relevance to oral bioavailability and blood-brain barrier (BBB) penetration [36,37]. The physico-chemical parameters analysed including molecular weight (MW), solvent accessible surface area (SASA) and octanol-water partition coefficient (QlogPo/w) are found in acceptable limit value, supporting favourable oral drug-likeness. The SASA values of the suggested drugs fall within the recommended range, implying suitable solubility and interaction potential with the biological membranes. The $QlogP_{o/w}$ values shows the moderate lipophilicity, a property essential for crossing biological hydrophobic barriers such as blood-brain barrier (BBB).

Key ADMET parameters were analyzed to assess the pharmacokinetic performance of diazepam and epicatechin. The QPlogBB values indicated stronger blood–brain barrier penetration for diazepam, consistent with its established CNS activity, while epicatechin also fell within an acceptable range, suggesting potential neurological applicability. Predicted MDCK permeability (QPPMDCK) showed high permeability for epicatechin and moderate permeability for diazepam, indicating efficient intestinal absorption. Both compounds demonstrated acceptable human serum albumin binding (QPlogKhsa), supporting favourable systemic distribution. Drug-likeness indices including ClogP and QPlogS, along with toxicity predictions, revealed suitable profiles and low toxicity risk for both molecules. However, predicted human oral absorption differed remarkably between the two compounds. Epicatechin exhibited 100% predicted oral absorption, indicating excellent permeability and solubility, whereas diazepam showed 52%, which remains within an acceptable range for oral administration [38,39].

$GABA_A$ receptors: The $GABA_A$ receptor, a major inhibitory neurotransmitter receptor in the central nervous system, regulates fast synaptic inhibition and maintains the balance between neuronal excitation and inhibition. Structural disruption or functional alteration of this receptor has been associated with several neurological and psychiatric disorders, including anxiety, epilepsy, schizophrenia and depression [40]. To investigate the ligand-receptor interactions, 3D structures of epicatechin (Fig. 6a), diazepam (Fig. 6b), GABA (Fig. 6c) and the $GABA_A$ receptor in *apo*-form (Fig. 6d) were used for molecular docking analysis. The optimized ligand geometries enabled evaluation of binding orientation, interaction profiles and binding affinity within the receptor binding pocket.

Docking results indicated stable ligand accommodation within the active-site cavity of the $GABA_A$ receptor, supported by favorable interaction energies and appropriate molecular orientation. Functional groups present in the ligands, particularly hydroxyl, amine and aromatic moieties, contributed to hydrogen bonding, electrostatic interactions and hydrophobic contacts with amino-acid residues in the receptor binding region. These interactions suggest structural compatibility between the ligands and the receptor's active site. The visualization of ligand–receptor complexes provide insight into molecular recognition and stabilization mechanisms, supporting the hypothesis that these compounds may influence GABAergic signaling pathways.

Ramachandran plot: The structural quality of the receptor model (PDB ID: 8BHK) was evaluated using a Ramachandran plot (Fig. 7). The energetically favourable backbone conformations were denoted by the colored region of the plot. The darker or reddish areas correspond to the most favoured regions, typically associated with stable secondary structure such as α-helices and β-sheets. And each black dot in the densely populated region represent an amino acid residue from a high-resolution protein structure. Their high density reflects that these backbone conformations are frequently observed in naturally occurring protein due to their low steric hindrance and acceptable intramolecular interactions. The light

TABLE-1
ADMET PROPERTIES PREPARED FOR DIAZEPAM AND EPICATECHIN

Compound name	mol MW	SASA	QPlogS	QPlogKhsa	QPlogHERG	QPPCaco	QPlogBB	QPPMDCK	Percent human oral absorption
Diazepam	302.24	517.529	-2.883	-0.342	-5.075	19.267	-2.38	6.925	52.192
Epicatechin	414.713	767.813	-8.557	2.059	-4.649	3404.348	-0.348	1859.584	100

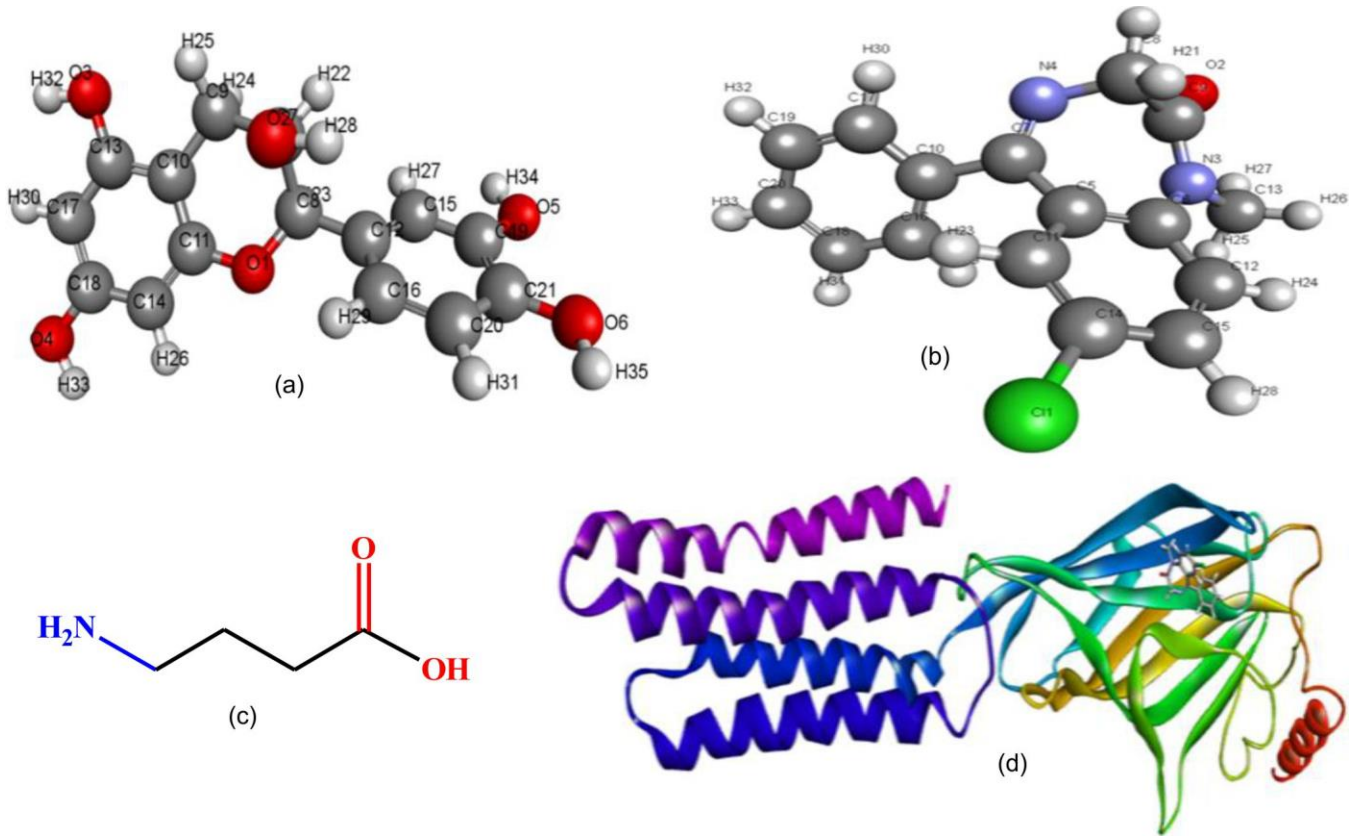

Fig. 6. (a) 3D representation of epicatechin, (b) 3D representation of diazepam, (c) 2D representation of $GABA_A$, (d) 3D representation of $GABA_A$ (γ-aminobutyric acid type A) receptors in apo form

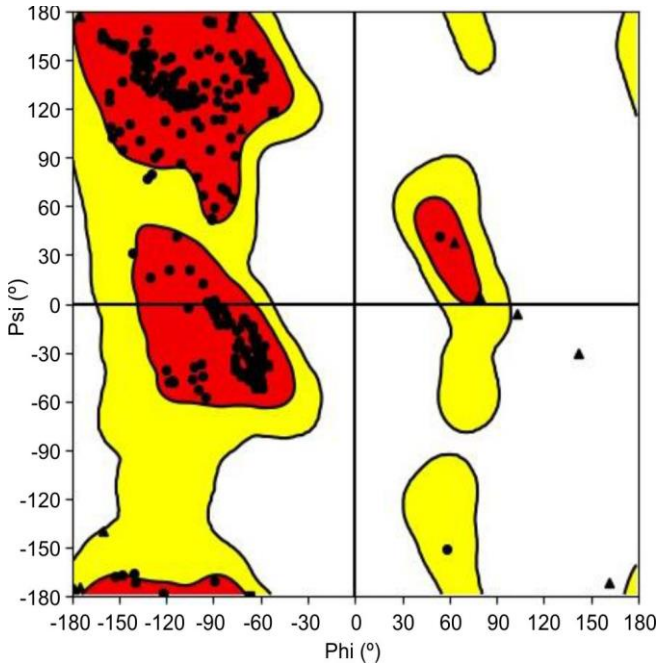

Fig. 7. Ramachandran plot shown the ordered and unordered regions

yellow areas, surrounding the core favoured regions, often observed in loops or structural junctions, representing allowed and less commonly adopted conformations. Whereas, the white or unshaded regions denote disallowed conformation, where the concurrent values of φ and ψ angles would produce steric clashes or energetically unfavorable interactions. The absence of black dots in this plot indicates that natural proteins very seldom adopt such conformations since they are structurally unstable or phsically constrained.

The minimal presence of residues in disallowed regions confirms good stereochemical integrity and conformational stability of the protein model, supporting its suitability for molecular docking analysis. Docking of epicatechin into the receptor binding pocket demonstrated favourable binding orientation and interaction stability. The hydroxyl functional groups of epicatechin contributed to hydrogen-bond interactions, while the aromatic rings enabled hydrophobic and π-interactions within the active site. These interactions indicate stable ligand–receptor complex formation and provide structural insight into ligand recognition and binding within the receptor binding domain.

Molecular docking study: In present work, the docking simulations were performed to assess the binding potential of selected drug candidate with the $GABA_A$ receptor (PDB ID:8BHK) using the extra precision (XP) docking protocol. The chosen drugs diazepam (a standard benzodiazepine) and (-)epicatechin (a naturally occurring flavonoid), were docked into the receptor's ligand binding domain. Both the drug molecule exhibited strong and stable binding conformation within the active site. The docking scores for diazepam and epicatechin were analysed as -5.204 kcal/mol and -4.216 kcal/mol, respectively (Table-2), reflecting favourable binding energies and strong affinity towards the $GABA_A$ receptor.

TABLE-2
PREDICTED DOCKING SCORE FOR $GABA_A$ RECEPTOR AND DRUG CANDIDATES

Compound ID	Compound name	Docking score	Hydrogen bonding & distance
3016	Diazepam	-4.216	105A, HIS: 2.10 Å
72276	Epicatechin	-5.204	105A, HIS: 1.98; 105A, HIS: 3.47; 162A, SER: 2.87; 163A, TYR: 1.70; 208A, THR: 2.81; 209A, SER: 3.26

The 2D interaction profiles (Fig. 8) show hydrogen bonds between the ligands and key active-site residues, represented by green dashed lines. Both diazepam and epicatechin formed hydrogen-bond interactions with HIS A:105, SER A:162, TYR A:163, THR A:208 and SER A:209, supporting stable ligand space within the binding pocket. Hydrophobic contacts, indicated by pink dashed lines, were observed with residues such as PHE A:103 and TYR A:213, contributing further to binding stabilization. In addition, π–π stacking interactions occurred between the aromatic rings of the ligands and aromatic residues in the receptor cavity, an important feature for molecular recognition within the $GABA_A$ binding site. The phenolic hydroxyl groups of epicatechin facilitated hydrogen bonding, whereas the aromatic framework of diazepam supported π-interactions consistent with classical benzodiazepine binding behaviour.

Impairment of $GABA_A$ receptor function is strongly associated with CNS disorders including epilepsy, Alzheimer's disease, Parkinson's disease and Huntington's disease [41-44].

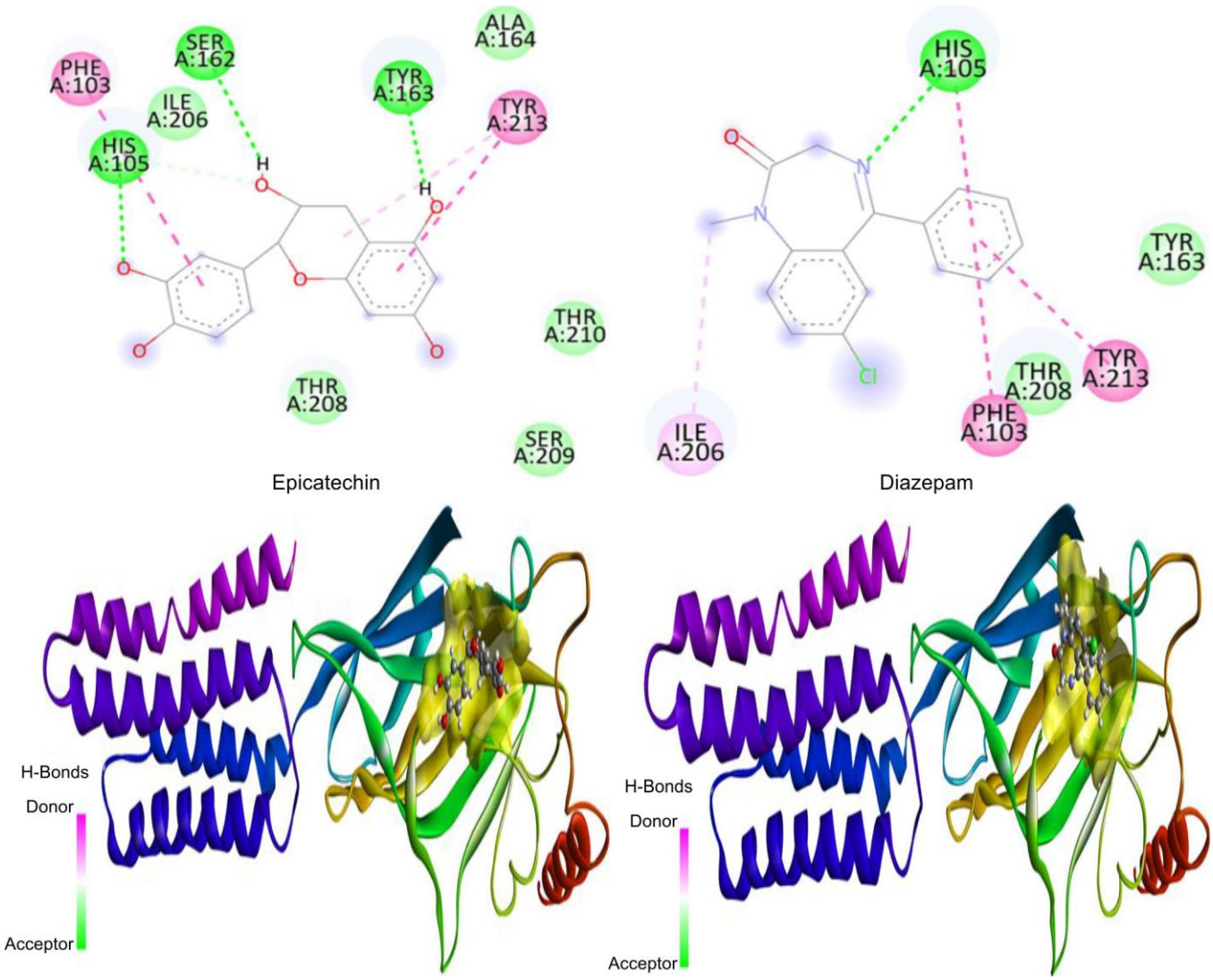

Fig. 8. 2D and 3D interaction poses between GABA protein and epicatechin and diazepam in the ligand-binding domain

Reduced GABAergic signalling leads to neuronal hyperexcitability, while conventional antiepileptic drugs such as diazepam and phenobarbital enhance inhibitory neurotransmission to restore balance [45]. Emerging evidence indicates that plant derived flavonoids including (-)-epicatechin, quercetin and kaempferol, can interact with $GABA_A$ receptors due to the structural similarities with benzodiazepines [46]. Beyond

receptor modulation, their phenolic structure enables antioxidant activity, helping mitigate oxidative stress implicated in neurodegeneration [47,48].

Conclusion

Preliminary phytochemical evaluation confirmed that the ethanolic extract of *Cassia fistula* L. seed contains diverse bioactive constituents. The isolated compound was characterised as (2*R*,3R)-2-(3,4-dihydroxyphenyl)-3,4-dihydro-2*H*-chromene-3,5,7-triol (epicatechin) based on physico-chemical parameters and comprehensive spectroscopic analyses. The melting point 238-239 ºC), molecular weight (290.08 g/mol) and molecular formula ($C_{15}H_{14}O_{16}$) were consistent with reported data. UV absorption maxima at 226.8 and 279.9 nm indicated a conjugated phenolic system typical of flavonoids. Structural confirmation was achieved through FT-IR, ^{1}H NMR and ^{13}C NMR studies. Chromatographic techniques, including TLC, HPTLC (R_f = 0.58) and HPLC (retention time ~3.865 min), verified the purity and identity of the isolated compound. *In silico* evaluation demonstrated favourable physico-chemical, pharmacokinetic and pharmacodynamic characteristics, supporting its compliance with drug-likeness criteria. Molecular docking analysis revealed stable binding of epicatechin within the $GABA_A$ receptor active site through hydrogen bonding, hydrophobic contacts, and electrostatic interactions. Epicatechin exhibited a stronger binding affinity (-5.204 kcal/mol) compared to diazepam (-4.216 kcal/mol) indicating enhanced receptor interaction. These findings suggest that epicatechin possesses promising GABAergic modulatory potential and may serve as a prospective candidate for the development of novel antiepileptic therapeutics.

ACKNOWLEDGEMENTS

The authors express their sincere thanks to their respective College Management for providing the necessary requirements for this research work.

CONFLICT OF INTEREST

The authors declare that there is no conflict of interests regarding the publication of this article.

DECLARATION OF AI-ASSISTED TECHNOLOGIES

During the preparation of this manuscript, the authors used an AI-assisted tool(s) to improve the language. The authors reviewed and edited the content and take full responsibility for the published work.

REFERENCES

1. M.M. Hasan, M.S. Hossain, M.A. Taher and T. Rahman, *Toxicol. Int.*, **28**, 155 (2021); https://doi.org/10.18311/ti/2021/v28i2/26775
2. W. Li, A. Maris, S. Melandri, A. Lesarri and L. Evangelisti, *J. Mol. Struct.*, **1296**, 136910 (2024); https://doi.org/10.1016/j.molstruc.2023.136910
3. A.A.H. Pinkey, Z.I. Khan, M.A. Taher and M.A. Soma, *Int. J. Med. Med. Res.*, **6**, 44 (2021); https://doi.org/10.11603/ijmmr.2413-6077.2020.2.11388
4. A. Rahman, M.M. Hasan, M.A. Taher and T. Muslim, *Banglades. Pharm. J.*, **23**, 141 (2020); https://doi.org/10.3329/bpj.v23i2.48334
5. M.A. Taher, A.A. Laboni, S.A. Shompa, M.M. Rahman, M.M. Hasan, H. Hasnat and M. Khan, *Chin. J. Anal. Chem.*, **51**, 100336 (2023); https://doi.org/10.1016/j.cjac.2023.100336
6. M.L. Gonzalez-Rivera, J.C. Barragan-Galvez, D. Gasca-Martínez, S. Hidalgo-Figueroa, M. Isiordia-Espinoza and A.J. Alonso-Castro, *Molecules*, **28**, 3457 (2023); https://doi.org/10.3390/molecules28083457
7. B.-J. Guo, Z.-X. Bian, H.-C. Qiu, Y.-T. Wang and Y. Wang, *Ann. N.Y. Acad. Sci.*, **1401**, 37 (2017); https://doi.org/10.1111/nyas.13414
8. F. Bourgaud, A. Gravot, S. Milesi and E. Gontier, *Plant Sci.*, **161**, 839 (2001); https://doi.org/10.1016/S0168-9452(01)00490-3
9. H.I.A. Boy, A.J.H. Rutilla, K.A. Santos, A.M.T. Ty, A.I. Yu, T. Mahboob, J. Tangpoong and V. Nissapatorn, *Digit. Chin. Med.*, **1**, 131 (2018); https://doi.org/10.1016/S2589-3777(19)30018-7
10. S.M. Mawalagedera, D.L. Callahan, A.C. Gaskett, N. Rønsted and M.R. Symonds, *Front. Ecol. Evol.*, **7**, 267 (2019); https://doi.org/10.3389/fevo.2019.00267
11. M.G. Moloney, *Trends Pharmacol. Sci.*, **37**, 689 (2016); https://doi.org/10.1016/j.tips.2016.05.001
12. A.G. Atanasov, S.B. Zotchev, V.M. Dirsch and C.T. Supuran, *Nat. Rev. Drug Discov.*, **20**, 200 (2021); https://doi.org/10.1038/s41573-020-00114-z
13. D.J. Newman and G.M. Cragg, *J. Nat. Prod.*, **83**, 770 (2020); https://doi.org/10.1021/acs.jnatprod.9b01285
14. C.R. McCurdy and S.S. Scully, *Life Sci.*, **78**, 476 (2005); https://doi.org/10.1016/j.lfs.2005.09.006
15. S.L. Jothy, Z. Zakaria, Y. Chen, Y.L. Lau, L.Y. Latha and S. Sasidharan, *Molecules*, **16**, 5268 (2011); https://doi.org/10.3390/molecules16065268
16. V.P. Kumar, N.S. Chauhan, H. Padh and M. Rajani, *J. Ethnopharmacol.*, **107**, 182 (2006); https://doi.org/10.1016/j.jep.2006.03.013
17. M.M. Pandey, S. Rastogi and A.K.S. Rawat, *Evid. Based Complement. Alternat. Med.*, **2013**, 376327 (2013); https://doi.org/10.1155/2013/376327
18. R.W. Mwangi, J.M. Macharia, I.N. Wagara and R.L. Bence, *Biomed. Pharmacother.*, **144**, 112240 (2021); https://doi.org/10.1016/j.biopha.2021.112240
19. A. Luximon-Ramma, T. Bahorun, M.A. Soobrattee and O.I. Aruoma, *J. Agric. Food Chem.*, **50**, 5042 (2002); https://doi.org/10.1021/jf0201172
20. T. Bhakta, P.K. Mukherjee, K. Mukherjee, S. Banerjee, S.C. Mandal, T.K. Maity, M. Pal and B.P. Saha, *J. Ethnopharmacol.*, **66**, 277 (1999); https://doi.org/10.1016/S0378-8741(98)00220-7
21. S.S. El-Saadany, R.A. El-Massry, S.M. Labib and M.Z. Sitohy, *Nahrung*, **35**, 807 (1991); https://doi.org/10.1002/food.19910350804
22. P. Daisy, K. Balasubramanian, M. Rajalakshmi, J. Eliza and J. Selvaraj, *Phytomedicine*, **17**, 28 (2010); https://doi.org/10.1016/j.phymed.2009.10.018
23. A. Roy, A. Khan, I. Ahmad, S. Alghamdi, B.S. Rajab, A.O. Babalghith, M.Y. Alshahrani, S. Islam and M.R. Islam, *Biomed Res. Int.*, **2022**, 5445291 (2022); https://doi.org/10.1155/2022/5445291
24. H. Hasnat, S.A. Shompa, M.M. Islam, S. Alam, F.T. Richi, N.U. Emon, S. Ashrafi, N.U. Ahmed, M.N.R. Chowdhury, N. Fatema, M.S. Hossain, A. Ghosh and F. Ahmed, *Heliyon*, **10**, e27533 (2024); https://doi.org/10.1016/j.heliyon.2024.e27533
25. L. Hu, Y. Luo, J. Yang and C. Cheng, *Molecules*, **30**, 1184 (2025); https://doi.org/10.3390/molecules30051184
26. K.N. Venugopala, *Asian J. Chem.* **37**, 2947 (2025); https://doi.org/10.14233/ajchem.2025.34966

27. M. Zahra, H. Abrahamse and B.P. George, *Antioxidants*, **13**, 922 (2024); https://doi.org/10.3390/antiox13080922
28. A. Ullah, S. Munir, S.L. Badshah, N. Khan, L. Ghani, B.G. Poulson, A.-H. Emwas and M. Jaremko, *Molecules*, **25**, 5243 (2020); https://doi.org/10.3390/molecules25225243
29. X. Zeng, W. Zhao, T. Zhang, L. Wang, G. Yang, Y.-K. Chen, Q. Hu and M. Miao, *Asian J. Chem.*, **25**, 6622 (2013); https://doi.org/10.14233/ajchem.2013.14399
30. S.K. Panda, L.P. Padhi and G. Mohanty, *J. Adv. Pharm. Technol. Res.*, **2**, 62 (2011); https://doi.org/10.4103/2231-4040.79814
31. M. Wink, *Medicines*, **2**, 251 (2015); https://doi.org/10.3390/medicines2030251
32. K. Agrawal, A. Joshi, S. Ghildiyal, M. Gautam, M. Gangwar, R. Goel and V. Joshi, *Med. Plant*, **6**, 138 (2014); https://doi.org/10.5958/0975-6892.2014.00482.1
33. R.V. Gottumukkala, N. Nadimpalli, K. Sukala and G.V. Subbaraju, *Int. Sch. Res. Notices*, **2014**, 628196 (2014); https://doi.org/10.1155/2014/628196
34. V.S. Sangeetha and C.R. Stella, *Acta Sci. Biol. Sci.*, **45**, e67455 (2024); https://doi.org/10.4025/actascibiolsci.v45i1.67455
35. A.J. Yusuf, M.I. Abdullahi, A.M. Musa, A.K. Haruna, V. Mzozoyana and A. Sanusi, *J. Basic Appl. Sci.*, **27**, 101 (2020); https://doi.org/10.4314/njbas.v27i2.14
36. K.M. Saravanan, H. Zhang, R. Senthil, Y. Wei, K.K. Vijayakumar, V. Sounderrajan, and H. Shakila, *J. Biomol. Struct. Dyn.*, **40**, 1970 (2022); https://doi.org/10.1080/07391102.2020.1834457
37. A. Antović, R. Karadžić, J.V. Živković and A.M. Veselinović, *Acta Chim. Slov.*, **70**, 634 (2023); https://doi.org/10.17344/acsi.2023.8465
38. S. Cheng and Y. Ding, *Curr. Computeraided Drug Des.*, **17**, 785 (2021); https://doi.org/10.2174/1573409916666200724153240
39. X. Zheng, C. Wang, N. Zhai, X. Luo, G. Liu and X. Ju, *Int. J. Mol. Sci.*, **22**, 9645 (2021); https://doi.org/10.3390/ijms22179645
40. F. Xiao, X. Ding, Y. Shi, D. Wang, Y. Wang, C. Cui, T. Zhu, K. Chen, P. Xiang and X. Luo, *Comput. Biol. Med.*, **169**, 107958 (2024); https://doi.org/10.1016/j.compbiomed.2024.107958
41. R.A. Bakay and A.B. Harris, *Brain Res.*, **206**, 387 (1981); https://doi.org/10.1016/0006-8993(81)90539-4
42. T. Aoyagi, T. Wada, M. Nagai, F. Kojima, S. Harada, T. Takeuchi, H. Takahashi, K. Hirokawa and T. Tsumita, *Chem. Pharm. Bull. (Tokyo)*, **38**, 1748 (1990); https://doi.org/10.1248/cpb.38.1748
43. N. Nishino, H. Fujiwara, S.A. Noguchi-Kuno and C. Tanaka, *Jpn. J. Pharmacol.*, **48**, 331 (1988); https://doi.org/10.1254/jjp.48.331
44. H. Ebato, T.N. Seyfried and R.K. Yu, *J. Neurochem.*, **40**, 440 (1983); https://doi.org/10.1111/j.1471-4159.1983.tb11302.x
45. G.J. Amabeoku, *Hum. Exp. Toxicol.*, **27**, 811 (2008); https://doi.org/10.1177/0960327108099538
46. N. Choudhary, K.R.V. Bijjem and A.N. Kalia, *J. Ethnopharmacol.*, **135**, 238 (2011); https://doi.org/10.1016/j.jep.2011.02.019
47. T.H. Costa Marques, C.H. Santos De Melo, R.B. Fonseca De Carvalho, L.M. Costa, A.A. De Souza, J.M. David, J.P. De Lima David and R.M. De Freitas, *Biol. Res.*, **46**, 231 (2013); https://doi.org/10.4067/S0716-97602013000300002
48. F. Zongo, C. Ribuot, A. Boumendjel and I. Guissou, *J. Ethnopharmacol.*, **148**, 14 (2013); https://doi.org/10.1016/j.jep.2013.03.080